



*Citation for published version:*

Makhlouf, N, Maskell, D, Marsh, A, Natarajan, S, Dabaieh, M & Afify, M 2019, 'Hygrothermal Performance of Vernacular Stone in a Desert Climate', *Construction and Building Materials*, vol. 216, pp. 687-696.  
<https://doi.org/10.1016/j.conbuildmat.2019.04.244>

*DOI:*

[10.1016/j.conbuildmat.2019.04.244](https://doi.org/10.1016/j.conbuildmat.2019.04.244)

*Publication date:*

2019

*Document Version*

Peer reviewed version

[Link to publication](#)

*Publisher Rights*

CC BY-NC-ND

**University of Bath**

**Alternative formats**

If you require this document in an alternative format, please contact:  
[openaccess@bath.ac.uk](mailto:openaccess@bath.ac.uk)

**General rights**

Copyright and moral rights for the publications made accessible in the public portal are retained by the authors and/or other copyright owners and it is a condition of accessing publications that users recognise and abide by the legal requirements associated with these rights.

**Take down policy**

If you believe that this document breaches copyright please contact us providing details, and we will remove access to the work immediately and investigate your claim.

# 1 **Hygrothermal Performance of Vernacular Stone in a Desert Climate**

2  
3 Nahla N. Makhoul<sup>1</sup>, Daniel Maskell<sup>2,\*</sup>, Alastair Marsh<sup>3</sup>, Sukumar Natarajan<sup>2</sup>, Marwa  
4 Dabaieh<sup>4,5</sup>, Mohamed Moemen Afify<sup>1</sup>

5  
6 <sup>1</sup>Department of Architecture, Faculty of Engineering, Cairo University, Egypt

7 <sup>2</sup>Department of Architecture and Civil Engineering, University of Bath, UK

8 <sup>3</sup>School of Civil Engineering, University of Leeds, UK

9 <sup>4</sup>Department of Urban Studies, Malmö University, Sweden

10 <sup>5</sup>Department of Architecture, Design and Media Technology, Aalborg University, Denmark

11  
12 *\*Corresponding author email: D.Maskell@bath.ac.uk*

## 15 **ABSTRACT**

16 Remote desert communities are often the most vulnerable to temperature extremes, as lack of  
17 access to reliable electricity prevents the use of active cooling or heating. Hence, there is a  
18 need to investigate how the building envelope itself can be used to passively regulate indoor  
19 environments. Readily available vernacular building materials in such areas are thought to aid  
20 in not only attenuating temperature swings but also moisture regulation, which improves  
21 comfort in a dry climate. Thus, the aim of this research is to investigate the  
22 hygrothermal properties of three different stone types commonly used as building materials in  
23 the Western Desert of Egypt: sandstone, limestone and, uniquely, Karshif, a rock rich  
24 in sodium chloride. The materials' thermal conductivity, moisture sorption and buffering,  
25 water vapour resistance, porosity distribution and phase composition are experimentally  
26 investigated. Our results show that the local perception of limestone buildings having poor  
27 indoor comfort, despite the material's superior thermal conductivity and specific heat capacity  
28 is only explainable through the relative superiority of sandstone and Karshif in moisture  
29 buffering. Vernacular materials need to be tested in environmental conditions representative  
30 of their local climate, rather than standardised conditions, as the latter may paint an incorrect  
31 picture of performance which, in the case of Karshif, led to partial dissolution under relative  
32 humidity of greater than 80%. However, testing under typical desert conditions demonstrates  
33 that both Karshif and sandstone are viable building materials that exhibit excellent moisture  
34 regulation behaviour. Since building materials in desert conditions may have to withstand  
35 atypical weather extremes, including rain, local materials need to be utilised within carefully  
36 designed wall assemblies or treated wall sections and, in the case of Karshif, not used in areas  
37 where relative humidity regularly reaches 80%. These findings are an important contribution  
38 in validating the performance of vernacular stone, and more widely, in demonstrating the  
39 importance of selecting appropriate testing conditions.

## 41 **KEYWORDS**

42 Hygroscopic, hygrothermal, Salt, Dynamic Vapour Sorption, sorption-desorption isotherm,  
43 Karshif, vernacular stone; Desert Architecture; Western Desert of Egypt

## 44 1 INTRODUCTION

45 Globally, the twin challenges of reducing energy use in buildings and improving the indoor  
46 environment have become core parts of both mandatory and voluntary design standards. It is  
47 well-known that heat and moisture transfer through the building's external envelope can have  
48 a passive effect in regulating the indoor environment and improving building energy  
49 efficiency [1]. Low carbon, natural materials – traditionally used for vernacular construction –  
50 often exhibit a greater ability to regulate the indoor environment, than modern conventional  
51 building materials [2]. In communities remote from the main urban conurbations, readily  
52 available vernacular building materials are therefore likely to be not only more suitable, but  
53 also a practical solution to ensuring good indoor thermal environments.

54 At the same time, there is growing concern around the long-term sustainability of modern  
55 building materials, which are often faster to build with and are perceived to be more durable,  
56 in remote communities. An unintended consequence of their use, arising from their poor  
57 thermal performance, is a rise in the installation and use of air-conditioners (see Figure 1).  
58 Their presence in a remote desert location, such as Siwa Oasis, is likely to exacerbate  
59 conditions if artificial conditioning becomes the primary means of obtaining thermal comfort.  
60 In fact, recent evidence of indoor surface temperatures crossing the contact pain threshold  
61 suggests that, in some instances, use of lightweight modern materials could result in extreme  
62 discomfort [3]. The rise in the use of modern materials also seems to have prompted changes  
63 in the use of vernacular materials. For example, in the Siwa region of Egypt, studied here,  
64 limestone walls are now built to 0.15m thickness[4] compared to the traditional thickness of  
65 0.40m, which would provide greater thermal mass [5].

66 In remote desert areas, vernacular materials are thought to aid in not only attenuating  
67 temperature swings but also moisture regulation, which is crucial given the dry climate. This  
68 occurs due to the materials' inherent hygroscopic properties, i.e., the sorption and desorption  
69 of moisture from the environment in periods of high and low relative humidity respectively.  
70 This is commonly referred to as moisture buffering, and can be understood as a process of the  
71 material "adapting" to the surrounding environment [6]. Materials with high moisture  
72 buffering capacity contribute towards regulating comfortable indoor environments in extreme  
73 weather conditions, with high cooling demand [7]. Hence, there is a need to investigate how  
74 construction materials, and thereby the building envelope itself, can be used to passively  
75 regulate indoor environments.

76 Earth based construction is well-known for its moisture buffering ability [8, 9, 10]. One of the  
77 benefits of moisture transfer between earth walls in hot climates is that when indoor humidity  
78 decreases, the release of moisture content from the wall can work to passively cool the air due  
79 to the latent heat of evaporation [6]. Although this property of earth has been attributed to the  
80 presence of clay minerals, anecdotal evidence has suggested that some stones could  
81 demonstrate similar behaviour due to their porosity structure. However, the interaction  
82 between the temperature and moisture performance of these materials has not been studied,  
83 especially for hot dry climates.

84



85 **Figure 1: AC units appear on building facades in Siwa Oasis (courtesy Mona El-Kabbany)**

86

## 87 **2 STUDY BACKGROUND AND AIM**

88 Local stones – often sandstone or limestone – are commonly used as construction materials in  
 89 many remote desert areas. In addition, Karshif, a building material unique to areas in the  
 90 Western Desert of Egypt including Siwa Oasis [11], Gara Oasis [12], and Baharia Oasis, is  
 91 also studied. Karshif is derived from the Miocene, Quaternary, and more recent salt lake  
 92 deposits [11]. It is composed of salt (sodium chloride) with a salty mud impurities. Walls are  
 93 usually built to a thickness of 0.3-0.6 m [4, 11] with a maximum thickness of about 0.8 m,  
 94 providing high thermal mass.

95 All three studied materials, limestone, sandstone and Karshif are sourced from the Gara Oasis.  
 96 The Gara Oasis is located to the north east of Siwa Oasis, at a distance of 120 km of direct  
 97 off-road access. Siwa Oasis is centred at 29° 120 N and 25° 530 E, in the north western part of  
 98 the Western Desert of Egypt. The region of Siwa Oasis, covering an area of 7800 km<sup>2</sup>, was  
 99 deemed as a “natural protectorate” in 2002, i.e. an area that requires special management and  
 100 protection [13]. A unique feature of this area are the four distinctive natural saline lakes along  
 101 with natural springs [11, 13, 14, 15]. The climate of the Siwa Oasis is classified as hot-arid,  
 102 with short winters and long summers. Climatological data shows a monthly average  
 103 maximum temperature of 31°C (Standard Deviation (SD) = 6.2) over the year, a monthly  
 104 average minimum temperature of 17.3°C (SD = 7) [16], and average monthly relative  
 105 humidity (RH) of 43.8% (SD = 7.1) [15]. Monthly maximum temperature could reach 38.8°C  
 106 in July and August [15, 17], while being dry at average minimum RH around 33% in May.  
 107 RH raise during winter period to reach 63% in January and December [17], while annual  
 108 average RH is 45 % [15]. From January until June precipitation could reach 2mm.  
 109 Evaporation ranges from 283 mm/month in July to 67 mm/month in December.

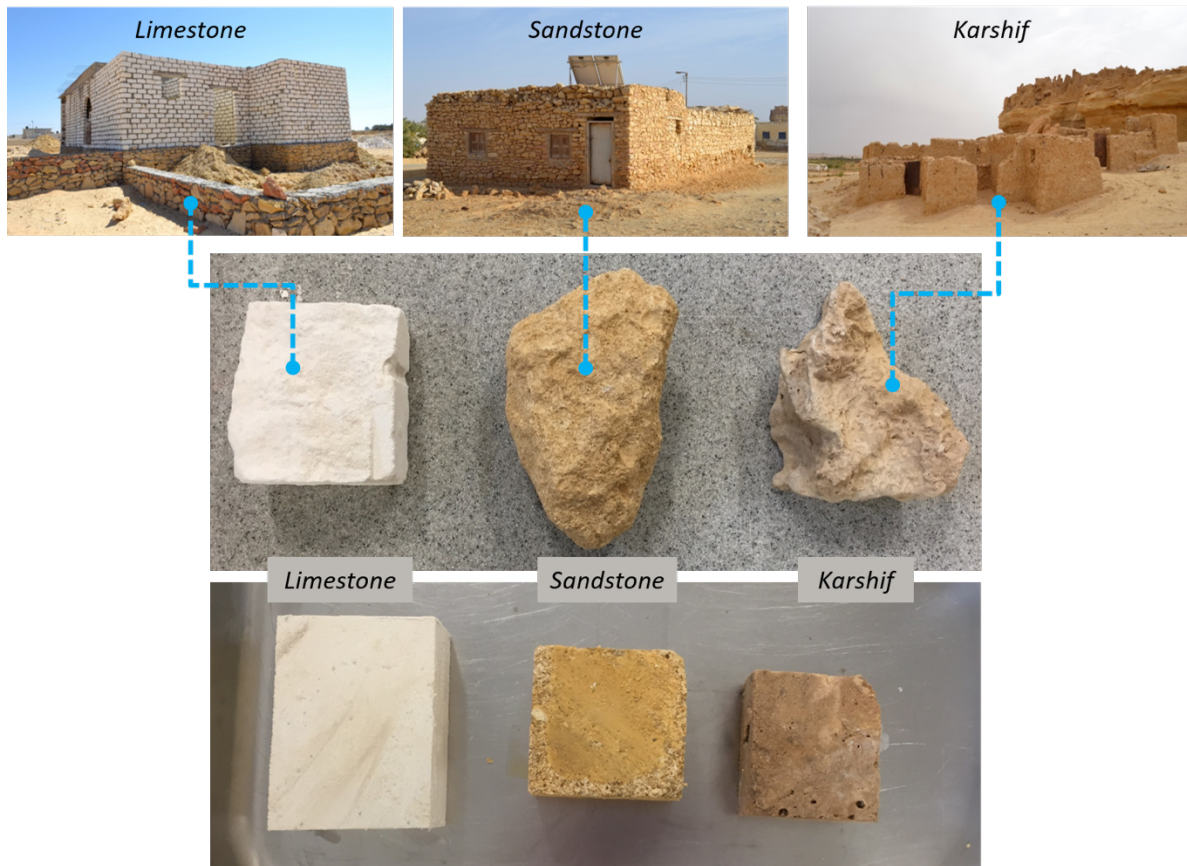
110 The aim of this study is to evaluate the mechanisms, and overall potential, of passive cooling  
 111 of three types of stone used for construction in the Western Desert. This is achieved by  
 112 characterising their material, thermal and hygroscopic properties and comparing with  
 113 evidence of in-situ performance. Our objectives are to physically and chemically characterise  
 114 the materials and establish the hygrothermal properties. These are demonstrated through  
 115 investigations of thermal conductivity, moisture sorption isotherms, moisture buffering and  
 116 water vapour resistance, under conditions representative of their intended desert environment.

117

## 118 **3 MATERIALS**

119 The three different stone types that are investigated are shown in Figure 2. Karshif can be  
 120 defined as an evaporite stone [11]. It is an evaporite deposit typically composed of Sodium  
 121 Chloride (NaCl) and secondary salt Potassium Chloride (KCl) with impurities of quartz,  
 122 feldspar, calcite and clay minerals [14]. Therefore, it is known to be very sensitive towards  
 123 excess water content, which could cause disintegration and deterioration.

124 Prior to testing, all specimen were cut into parallelepiped rectangular and uniform shapes in  
125 order to have flat surfaces. Specimen were left to dry in 80 °C oven for at least one week, then  
126 left in a climate controlled room at 20±2 °C and 50±2 %RH.



127  
128 **Figure 2: Illustration of the chosen building materials based on construction typologies in Gara Oasis**  
129 **(upper), Material samples before (middle) using water saw to cut into parallelepiped shape (lower)**

130

## 131 4 METHODS

132 Each of the stone types were experimentally tested three times, to determine their phase  
133 assemblages, physical and hygrothermal properties, using the following methods.

### 134 4.1 Phase Characterisation

135 Powder X-ray diffraction (PXRD) analysis was used to identify phases with a Bruker D8  
136 Advance instrument using monochromatic CuK $\alpha$ 1 L3 ( $\lambda = 1.540598 \text{ \AA}$ ) X-radiation and a  
137 Vantec superspeed detector. A step size of 0.023 °2 $\theta$  and step duration of 0.2 seconds were  
138 used over a range of 5 – 80 °2 $\theta$ . Phase identification was done using Bruker EVA software.  
139 Powder was produced by manually crushing samples using mortar and pestle, and was  
140 prepared for XRD by pressed glass slide method.

### 141 4.2 Physical Characterisation

142 Specific surface area was measured using the BET [18] method for nitrogen gas adsorption,  
143 with a Micromeritics 3flex Surface Characterization Analyzer. Three samples of each material  
144 were tested, with a sample mass of approximately 0.75±0.05 g. All samples were dried in a  
145 105 °C oven for 24h, and then dried for a further 24h under a nitrogen atmosphere at 105°C in  
146 a degassing unit (Micromeritics FlowPrep 060).

147 An Autopore Mercury Porosimetry (PASCAL 440, Thermo Scientific) was used to determine  
148 the porosity size distribution and average pore diameter of the materials. Three samples of  
149 each material were tested. Before testing, samples were dried in 105°C oven for at least 24h  
150 until constant mass was achieved. Samples were tested in solid state, with a sample mass of  
151 approximately 0.6 g, at temperature of 21±2 °C.

### 152 **4.3 Hygrothermal Properties**

#### 153 **4.3.1 Thermal properties**

154 The thermal properties were measured using ISOMET 2114, a transient plane source device,  
155 and using a surface probe IPS 1105. A flat surface of at least 60mm diameter is satisfactory  
156 for the probe, with a minimum thickness of the material to be 20mm. Non-homogeneity and  
157 anisotropy were overcome through testing three specimens for each material and ten repeats  
158 of the thermal conductivity measurement (i.e. 90 readings in total). This method's validity for  
159 small samples has been previously verified [19]. Measures of thermal conductivity,  $\lambda$   
160 (W/mK), thermal diffusivity (m<sup>2</sup>/s), and volume heat capacity (J/m<sup>3</sup>K) were obtained.

#### 161 **4.3.2 Dynamic Water Vapour Sorption (DVS) test**

162 The study followed BS EN ISO 12571:2013, using the climatic chamber method. A Dynamic  
163 Vapour Sorption (DVS) machine was used to produce a continuous isotherm for the climatic  
164 chamber method on sample masses ranging 45-80 mg. In order to ensure materials had 0%  
165 moisture content at the beginning of a test, specimens were dried in an oven at 105 °C until  
166 constant mass was recorded and then held for 360 min at 0% humidity at the set temperature.  
167 RH was set to increase from 0-95% and then back to 0% with 5% step change at a constant  
168 temperature. The step change is triggered when the gradient of mass change with respect to  
169 time (dm/dt) <0.002 wt.%/min. For each step, the moisture balance was considered to be  
170 reached if the change in mass did not raise more than 0.002% per minute.

171 To investigate the appropriateness of the ISO 12571 standard for observed environmental  
172 conditions of the region, the steady state temperature was varied. The objective was to  
173 determine the materials' performance with mean summer peak (38.8°C) through the hottest  
174 months in summer (July/August) and maximum summer peak that could reach 44°C, and to  
175 examine their response within). To allow for a comparison to the ISO standard, the full RH  
176 cycle (0-95%) was applied at 23°C and 38°C for the three materials. Additionally, to reflect  
177 realistic RH of the region each material was tested for RH 25-65% at 23°C, 38°C and 48°C  
178 over five cycles.

#### 179 **4.3.3 Water Vapour Resistance**

180 BS EN ISO 12572:2016 was followed to determine water vapour resistance of the three  
181 materials. Both dry cup and wet cup methods were applied. Three samples of each material  
182 were tested. For the dry cup, silica gel was used to provide 0% RH. For the wet cup, a  
183 saturated salt solution using potassium nitrate (KNO<sub>3</sub>) was used to provide 94% RH. All  
184 samples were left in a climate chamber at 23°C and 50% RH until constant mass change was  
185 achieved. Daily weight measurements were taken using OHAUS scale with readability up to  
186 0.01g.

#### 187 **4.3.4 Moisture Buffering Value (MBV)**

188 Following preparation, specimens were sealed on 5 faces using aluminium tape leaving one  
189 exposed surface. Due to the irregularity of the source rock, they were cut to provide the  
190 maximum possible surface area.

191 The standard NORD test [20] was used which exposed the materials for 8 hours at 75% RH  
192 and 16 hours 33% RH both at 23°C in an environmental chamber. A screen was placed  
193 around the mass balance to minimize the influence of air movement over the surface of the

194 specimens during testing. An anemometer was used to measure wind speed at the specimen  
 195 surface and was found to be an average of 0.1 m/s. All materials were weighed constantly on  
 196 scales during testing. This method allows for the calculation of the Moisture buffering value  
 197 (MBV) using the following equation (1):

198

199

$$MBV = \frac{\Delta m}{A \cdot \Delta RH} \quad (1)$$

200

201 While  $\Delta m$  is the difference as an average of the last four cycles between initial mass  $m_0$  and  
 202 maximum mass change  $m_8$  at 8 hours in high RH,  $A$  is exposed area of the material and  $\Delta RH$  is  
 203 the difference in RH between high and low.

204

## 205 5 RESULTS

### 206 5.1 Phase characterisation

207 A distribution of the mineralogical composition was found throughout the material samples,  
 208 as summarised in Table 1. At least two samples of each material were analysed, and so the  
 209 consistency of each phase's presence has been stated for each material.

210 Among the phases present were those expected to have a weak or negligible influence on  
 211 hygrothermal interactions, including silicas and carbonates. Quartz was also present in all  
 212 samples, with a trace amount of cristobalite found in some of the Karshif samples. Calcium  
 213 carbonates of some variety were present in all the materials, mostly calcite and dolomite.  
 214 Also found were phases expected to exert a strong influence on hygrothermal interactions:  
 215 halite (NaCl salt), clay and sulfates. Halite was present to some extent in all samples, as  
 216 expected of materials found from around the salt lake area. Calcium sulfates were present to  
 217 some extent in all the material types except limestone. A range of hydration states were found,  
 218 from dehydrated (anhydrite) to partially hydrated (calcium sulfate hydrate) to fully hydrated  
 219 (gypsum). These observations are in broad agreement with Rovero et al. [14] who concluded  
 220 Karshif to be an evaporite deposit composed of NaCl and secondary salt KCl with impurities  
 221 of quartz, feldspar calcite and clay minerals.

222 A clay mineral was present in some of the Karshif and sandstone samples - given that a soil in  
 223 this environment would be classified as an Aridisol, this clay mineral is likely to be kaolinite  
 224 [22].

225

**Table 1: Phase composition**

Phase	Formula	Karshif	Sandstone	Limestone
Quartz	SiO <sub>2</sub>	●	●	●
Cristobalite	SiO <sub>2</sub>	⊙	○	○
Dolomite	CaMg(CO <sub>3</sub> ) <sub>2</sub>	●	●	○
Calcite	CaCO <sub>3</sub>	●	○	●
Aragonite	CaCO <sub>3</sub>	○	○	⊙
Halite	NaCl	●	●	●
Anhydrite	CaSO <sub>4</sub>	●	○	○
Calcium Sulphate Hydrate	CaSO <sub>4</sub> ·0.67H <sub>2</sub> O	⊙	●	○
Gypsum	CaSO <sub>4</sub> ·2H <sub>2</sub> O	⊙	●	○
Kaolinite	Al <sub>2</sub> Si <sub>2</sub> O <sub>5</sub> (OH) <sub>4</sub>	⊙	●	○

● = always found, ⊙ = sometimes found, ○ = not found.

226

227 **5.2 Physical Characterisation**

228 Table 2 presents specific surface area and porosity results for BET and Mercury Intrusion  
 229 Porosimetry (MIP) tests respectively. The three materials had a relatively small average  
 230 specific surface area (1-3 m<sup>2</sup>/g). However, Karshif had a larger average specific surface area  
 231 than sandstone and limestone. This indicates that Karshif has the potential to adsorb a greater  
 232 quantity of adsorptive (such as moisture) from the surrounding environment, compared to  
 233 sandstone and limestone.

234  
 235 Regarding porosity, limestone had the highest (by skeletal density) amongst the three  
 236 materials, followed by sandstone and then Karshif. Regarding pore size distribution, Karshif  
 237 had a comparable pore surface area to limestone and sandstone, but a significantly lower  
 238 average pore diameter. This would suggest that the size distribution of porosity in the Karshif  
 239 tended towards smaller pores compared to those in the sandstone, and much smaller than  
 240 those in limestone.

241 **Table 2. Physical Properties**

Analysis	Karshif	Sandstone	Limestone
Porosity (by skeletal density) (%)	21.29	27.10	31.70
Bulk density (g/cm <sup>3</sup> )	1.97	1.82	1.71
Pore surface area (m <sup>2</sup> /g)	4.66	4.71	3.47
Average pore diameter (nm)	74	172	335
Average specific surface area (m <sup>2</sup> /g)	3.0	1.8	1.7

242

243 **5.3 Hygrothermal Properties**

244 The mean of all hygrothermal results are presented in Table 3. The coefficient of variation for  
 245 the thermal conductivity and specific heat capacity were all less than 5% and the coefficient  
 246 of variation for the water vapour resistance factor and moisture buffering value are presented  
 247 in brackets.

248

249

**Table 3 Mean Hygrothermal properties**

Sample	Thermal Conductivity* (W/mK)	Specific heat capacity* (kJ/kgK)	Water vapour resistance factor - "Wet" cup (μ value)	Water vapour resistance factor - "Dry" cup (μ value)	Moisture Buffering Value (g/m <sup>2</sup> RH%)
Karshif	1.62	0.71	3.11 (13.8%)	15.77 (9.1%)	3.48 (12.3%)
Sandstone	1.11	0.75	13.81 (11.4%)	22.81 (13.7%)	3.00 (10.5%)
Limestone	0.70	0.82	6.20 (15.4%)	13.99 (5.1%)	2.30 (11.4%)

250 Coefficient of variation: <5% for columns with \*; other columns as indicated in brackets.

251

252 **5.3.1 Thermal Properties**

253 Table 3 demonstrates that limestone had the lowest thermal conductivity and the highest  
 254 specific heat capacity among the three materials tested. These correspond to high thermal  
 255 resistance (hence heat or coolth loss) and high thermal mass respectively, both highly  
 256 desirable thermal properties in building materials. Dabaieh et al. [12] also reported thermal  
 257 conductivity of Karshif to range between 1.65 to 2.35 W/mK, which indicates the variability  
 258 of performance of natural building materials, and the difficulties of considering thermal  
 259 performance in isolation.

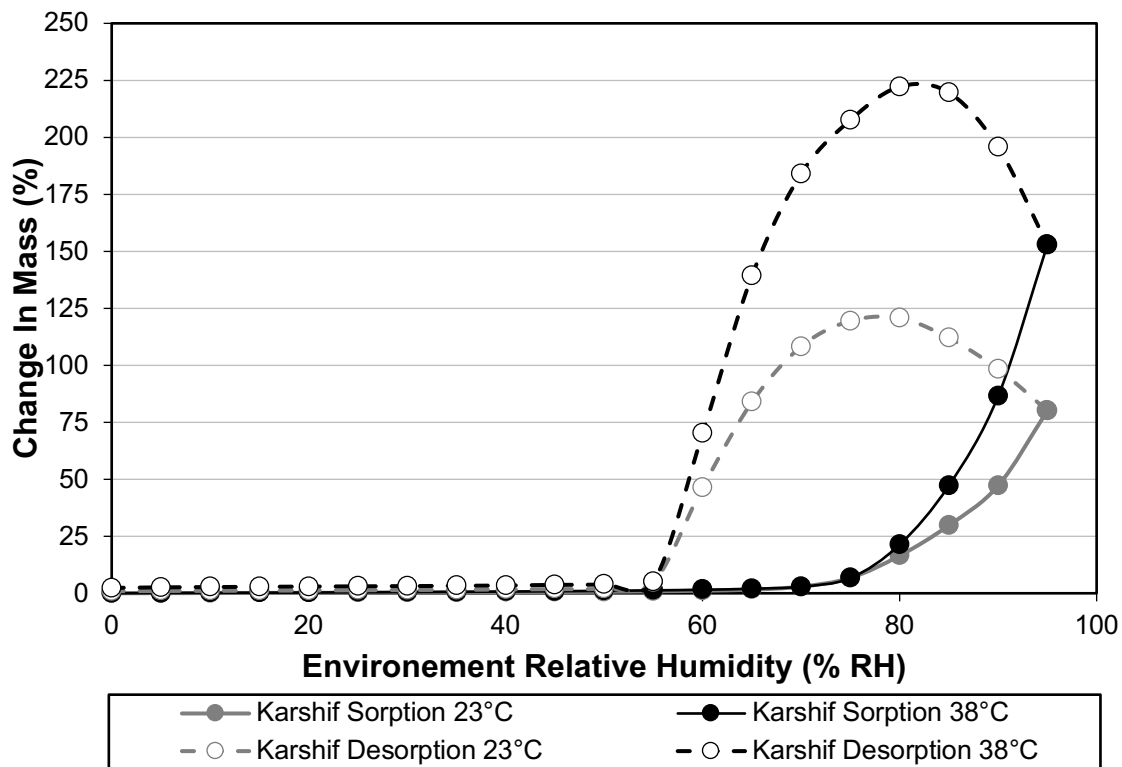
260

### 261 5.3.2 Dynamic Vapour Sorption (DVS)

262 The sorption and desorption of the different materials are presented in Figures 3 and 4.  
263 Karshif shows distinctly different behaviour compared to sandstone and limestone, with  
264 respect to both adsorption and desorption. It continues to increase in mass weight even after  
265 RH drops down, with mutually consistent results at both 23°C and 38°C.

266 The maximum change in mass for both sandstone and limestone is 2.6 % but Karshif, adsorbs  
267 80% and 150% at 23°C and 38°C respectively. In addition, Karshif sorption isotherm (Figure  
268 3) indicates a large hysteresis area between 55-95% RH, while limestone and sandstone  
269 (Figure 4) show very limited hysteresis within this same range. Pictures obtained from the  
270 built-in camera on the DVS demonstrate that a drop of water developed on top of the Karshif  
271 sample until reaching a dissolution point at around 75-78% RH, after which dissolution  
272 occurred (Figure 5). This leads to an atypical desorption curve as the liquid water remains  
273 present on the scales.

274

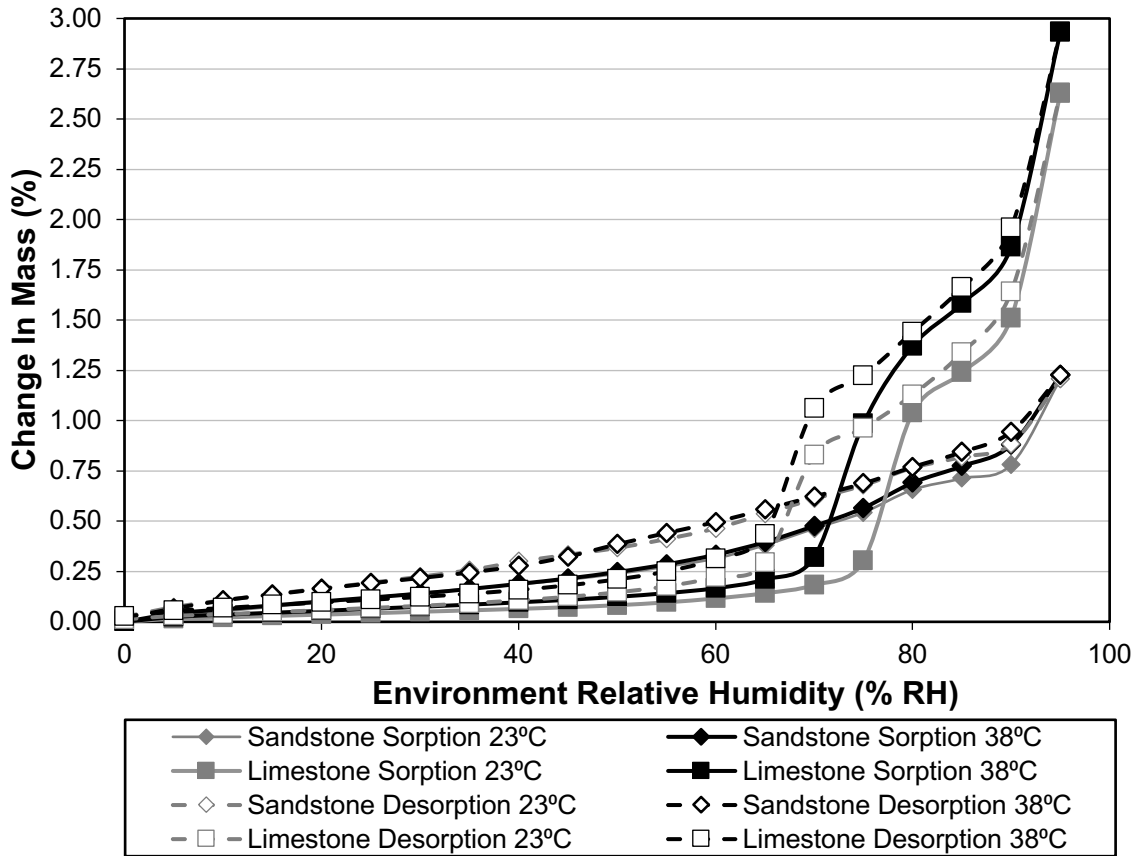


275

276

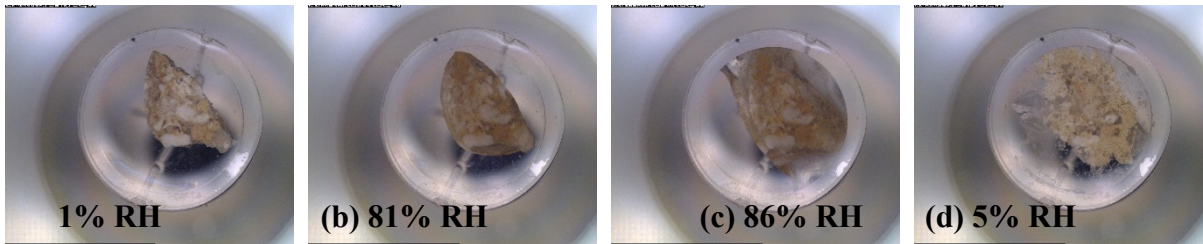
Figure 3: Combined moisture sorption isotherm for Karshif, 0-95% RH at 23°C & 38°C

277



279  
 280  
 281  
 282  
 283  
 284

Figure 4: Combined moisture sorption isotherm for Sandstone and Limestone, 0-95% RH at 23°C & 38°C



285  
 286  
 287  
 288  
 Figure 5: Period recorded pictures for Karshif sample using DVS built-in camera for full cycle test 0-95% RH at 23°C. (a) Start of sorption test at 1% RH Sample is dry. (b) A drop of water on top of a sample at 81% RH. (c) Material dissolved in water at 86% RH. (d) Dry sand/clay left after desorption at 5% RH.

289 **5.3.3 Water Vapour Resistance**

290 The “wet” and “dry” cup water vapour transmission are presented in Table 4. During “wet”  
 291 cup testing for the Karshif sample, a crystalline growth was observed (Figure 7). This is  
 292 comparable to the observations from the DVS, where at high RH (as with the wet cup) the  
 293 material dissolves, allowing crystal regrowth at the material surface when the environmental  
 294 RH returns to 50%.

295 Sandstone shows high vapour resistance factor at both dry and wet cup tests. Karshif shows  
 296 the least water vapour resistance factor in wet cup test. Accordingly, moisture can easily

327 penetrate into the material in a high humidity environment. Due to its phase composition,  
328 water is held in its cavities causing partial dissolution of the material if high humidity persists,  
329 and then acts to humidify the surrounding dry atmosphere when RH drops.  
330



331  
332 **Figure 6: Images of Karshif when: salt forms around the seal during wet cup test (left) and the inner**  
333 **exposed surface is at the point of dissolution causing a muddy appearance (right).**

## 334 6 Analysis and Discussion

335 The results have indicated the varying characteristics and hygrothermal properties for  
336 different vernacular building materials. Al-Taweel [5] and Petruccioli & Montalbano [23],  
337 both comment on the improved thermal comfort of Karshif buildings in the Siwa region. In  
338 contrast, our results (Table 5) indicate that buildings built with Karshif should perform the  
339 worse thermally than sandstone and limestone constructions, indicating that other material  
340 factors may play a significant role. The hygrothermal performance is dependent on the  
341 mineralogical composition, as well as the physical properties. The unique characteristics of  
342 the Karshif vapour sorption led to further analyses into real world performance below.  
343

### 344 6.1 Effect of physio-chemical composition on hygrothermal performance

345 The phases of most interest in these materials are those which are likely to have strong  
346 interactions with moisture. This is either due to their ability to undergo a  
347 dissolution/precipitation process (halite), a hydration/dehydration process (calcium sulphates)  
348 or having a large charged specific surface area (clay).  
349

350 Previous investigation of the geological formation immediately around the Gara Oasis have  
351 found limestone to contain both kaolinite and gypsum [24] The co-existence of halite with  
352 calcium sulphate phases in various states of hydration is of particular interest, given that  
353 dehydration transformations in calcium sulphates are facilitated by the presence of salt water  
354 [25]. From the different mineralogical constituents (Table 1), it is observed that Karshif and  
355 Sandstone contain halite (NaCl salt), calcium sulphates and clay, whereas limestone does not.  
356 At the same time, these stones have a significantly higher moisture buffering value. As  
357 identified in Figure 3, Karshif quickly increases in mass at 70-75% RH and a thin layer of  
358 liquid (assumed to be saturated salt solution) condenses around the sample and causes  
359 dissolution of the halite within the stone. The continuous increase in mass for Karshif even  
360 after RH decreases is due to the condensation of water onto the samples, effectively making a  
361 salt solution. Saturation humidity for sodium chloride is 76% [26] which is comparable to the  
362 humidity when Karshif sample starts to dissolve. The impact of the dissolution of halite has  
363 been observed within the moisture sorption curves (Figure 3) as well as the “wet” cup test  
364

335 (Table 6). Whereas the “dry” cup test and moisture buffering test never expose the material to  
336 relative humidities significant for dissolution.

337 Both the thermal and moisture sorption relate to the physical and chemical characteristics of  
338 the material. There is a correlation between the bulk density and pore size with the thermal  
339 conductivity and specific heat capacity. However, none of these materials provide significant  
340 resistance to thermal transmission and have almost similar specific heat capacity. Given the  
341 dry environment of a desert, moisture buffering properties are an important factor to provide  
342 indoor thermal comfort as this allows the regulation of humidity levels in the indoor  
343 environment when humidity is low.

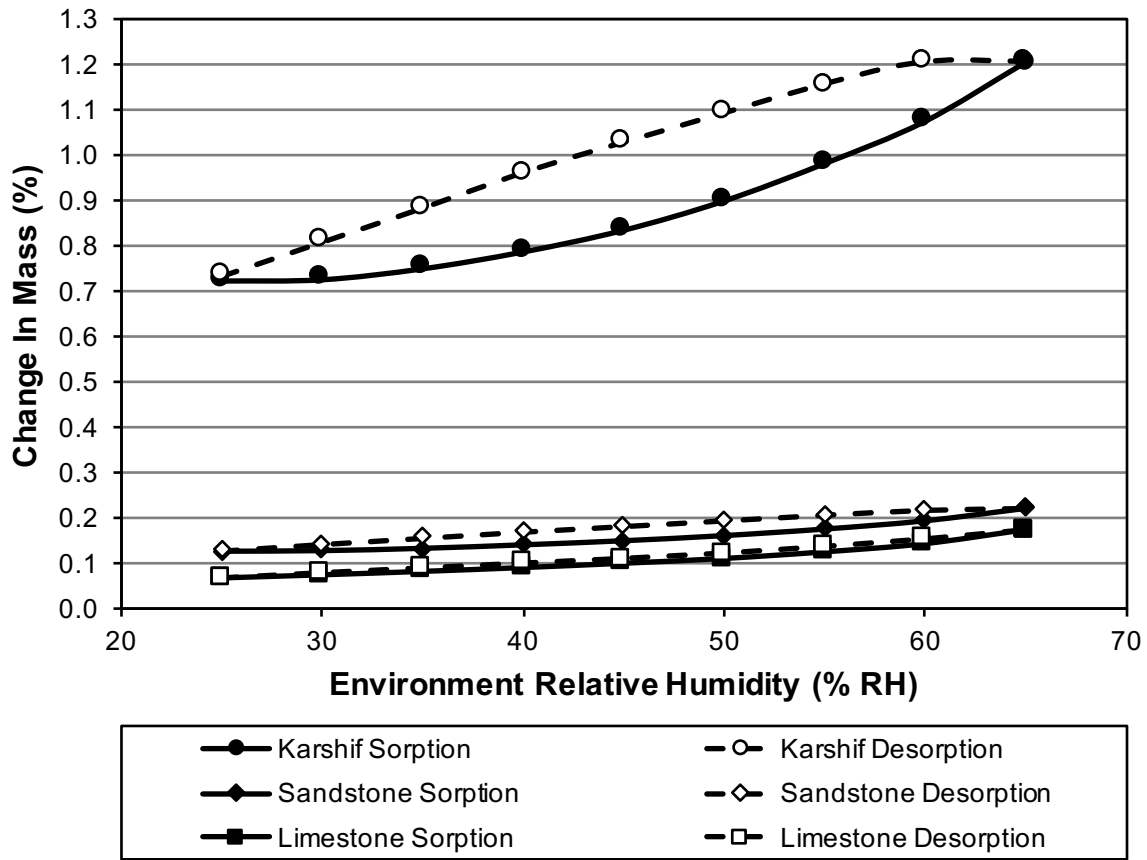
344 Limestone seems to have the best thermal properties among the three materials, attributed to  
345 its higher porosity and larger pore diameter. These porous characteristics of the limestone help  
346 not only to provide better insulative properties but also higher moisture sorption  
347 characteristics and lower vapour resistance compared to sandstone and Karshif when only  
348 considering the “dry” cup test. Although limestone has the better thermal properties of the  
349 three materials, the performance is not that significant when considering the multiple criteria  
350 of a material’s role in regulating the indoor environment [27], specifically the role moisture  
351 sorption and buffering can have on the thermal performance and comfort.

## 352 **6.2 Development of appropriate sorption isotherm for context**

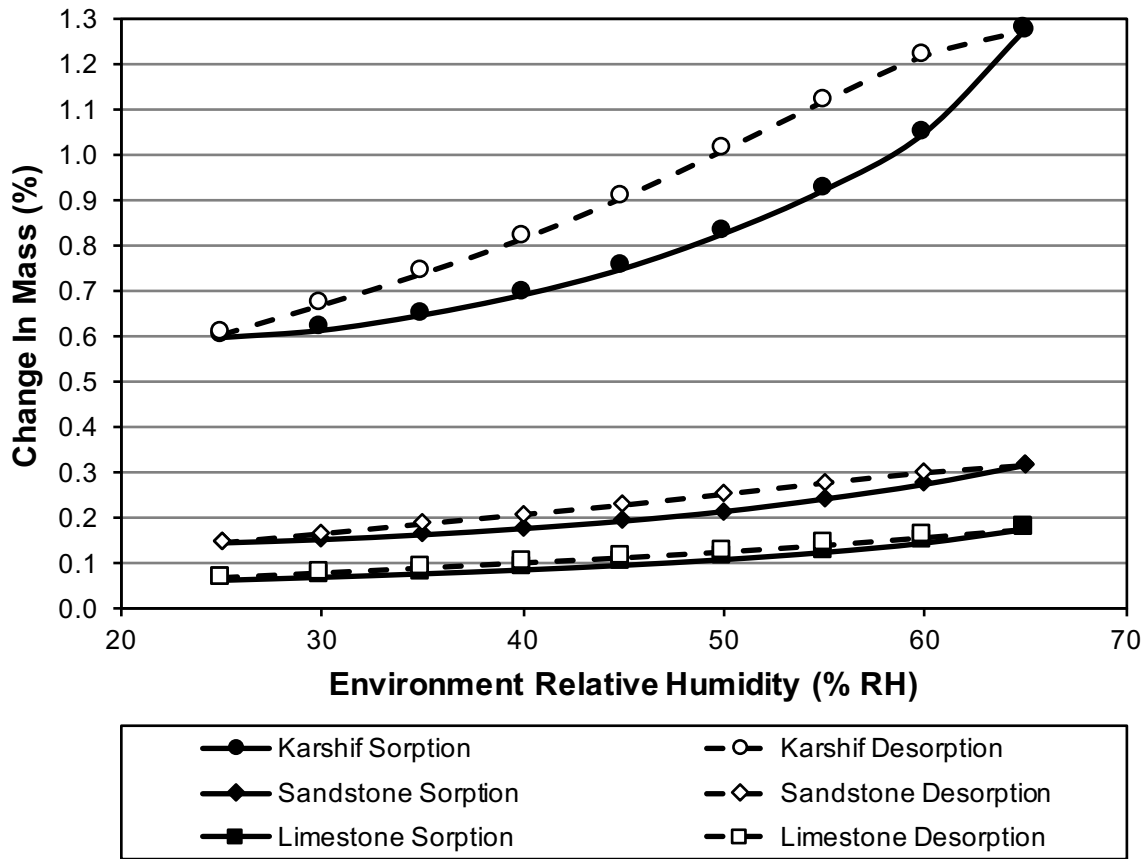
353 Various adsorption isotherm typologies were identified by Sing et al. [28], which have since  
354 been used to analyse the adsorption of water vapour for a variety of materials [29, 30, 31].  
355 Given the range of partial pressures used in these tests, it was not possible to state the  
356 isotherm type with confidence. However, comparison of certain features in these isotherms  
357 (Figure 3 and 4) with those of the established typologies can be used to interpret the materials’  
358 behaviours. Limestone’s sorption isotherm showed very little hysteresis on desorption, which  
359 is typical for non-porous or macroporous materials. This suggests that limestone exhibited  
360 neither a large extent of mesoporosity, nor a strong adsorbent-adsorbate interaction.  
361 Consequently, limestone was able to release all the adsorbed moisture content back to the  
362 surrounding environment. Sandstone demonstrated a small extent of hysteresis, which  
363 indicates a greater extent of mesoporosity, and/or an adsorbent-adsorbate interaction,  
364 compared to limestone. This interpretation is supported by the smaller average pore diameter  
365 (Table 2) and wider prevalence of moisture-interacting phases (Table 1) in sandstone  
366 compared to limestone. Karshif demonstrated a very strong hysteresis effect. This was largely  
367 attributed to the moisture’s interaction with halite, as material dissolution was visibly  
368 observed (Figure 5). A higher extent of mesoporosity (Table 2) and presence of other  
369 moisture-interacting phases (Table 1) could also have contributed to this.

370 The phenomenon of dissolution of these materials is not commonly observed in the buildings  
371 in the Gara Oasis, unless for Karshif at atypical devastating heavy rain occasions, like what  
372 have been observed in 1928, 1930, 1970, 1982 [32], and in 1985 [5] in Siwa Oasis and during  
373 1980’s in Gara Oasis [33]. This could indicate that this testing approach is not appropriate for  
374 the true typical moisture sorption-desorption isotherm behaviour, as the desorption curve is  
375 impacted by the presence of a salt solution that would not typically be observed. The typical  
376 tested conditions, following ISO 12571:2013, of the vapour sorption (0-95%) and desorption  
377 isotherm (23 °C) do not represent the conditions observed in the Gara Oasis where these  
378 materials are used. Cycling between 0 and 95% RH has also shown to produce abnormal  
379 desorption patterns that would not be typically induced. Therefore, a development of the  
380 standard vapour sorption testing is required to represent local conditions. The three materials  
381 have been exposed to five repeated cycles of 25-65% RH at 23 °C, 38 °C, 48 °C as represented

382 in Figure 7, 8 and 9 respectively. This allows for a greater understanding of the material's  
383 performance under real conditions, which is not achieved when testing solely at 23 °C.

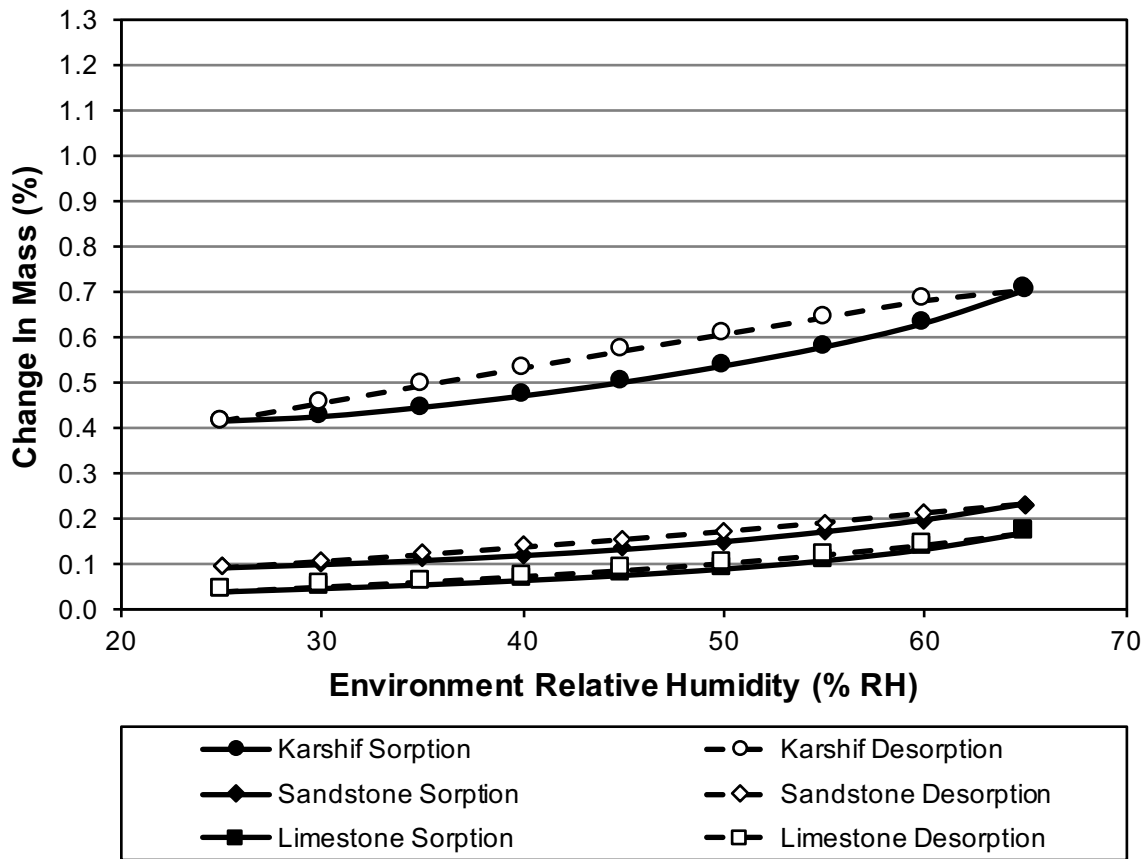


384  
385 **Figure 7: Final cycle of moisture sorption isotherm between 25-65% RH at 23°C**



386  
387

Figure 8: Final cycle of moisture sorption isotherm between 25-65% RH at 38°C

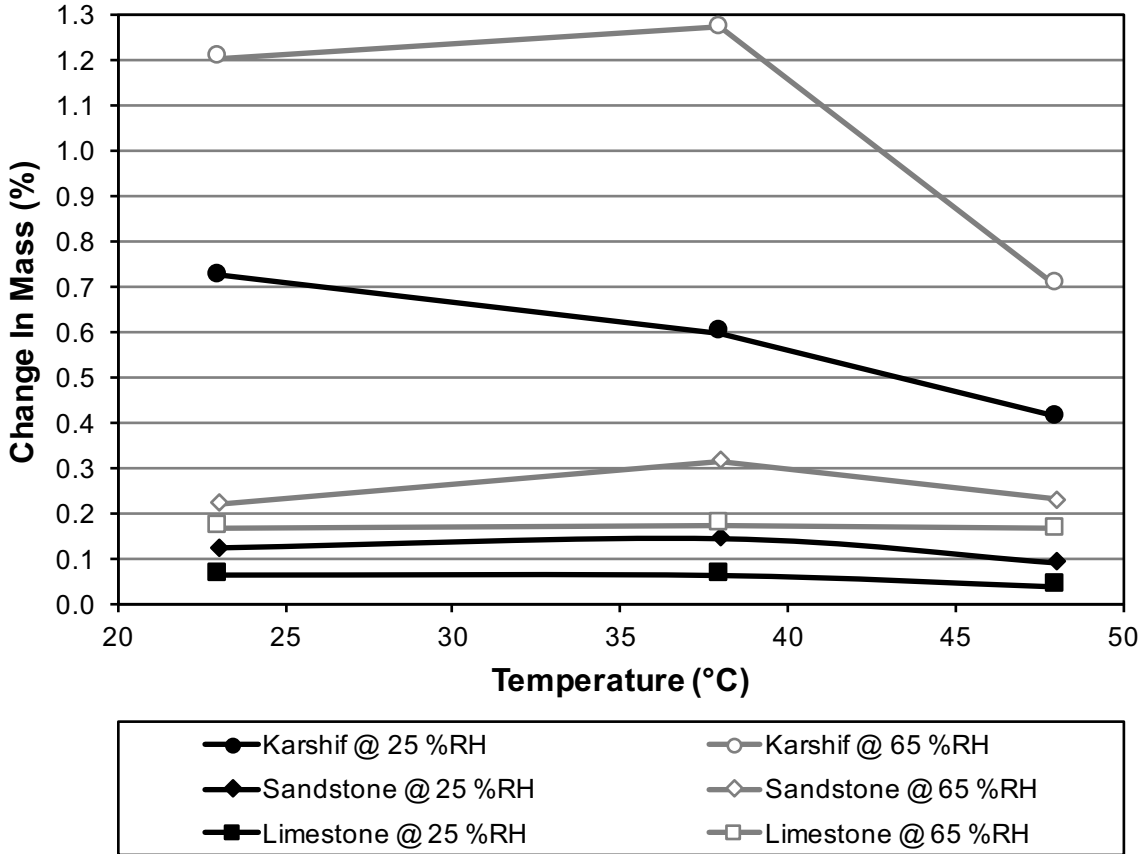


388  
389

Figure 9: Final cycle of moisture sorption isotherm between 25-65% RH at 48°C

390  
391  
392  
393  
394  
395  
396  
397  
398  
399

The change in the environmental temperature fundamentally allows for varying absolute mass of moisture to be stored in the air. Therefore, a consistent RH for varying temperatures does not result in isobaric conditions. In addition to a differing partial pressure, varying temperature may affect each material differently, in some cases resulting in structural changes and reactions (such as salt dissolution) to occur at different temperatures. This will have the impact of changing the amount of moisture a material can hold. Variation in adsorption capacity is observed in Figure 3 and 4 for the full cycle and Figure 7, 8 and 9 for the reduced cycle. The change in sorption capacity at 25% and 65% RH can be observed from Figure 10.



400  
401  
402  
403  
404  
405  
406  
407  
408  
409  
410  
411

Figure 10: Impact of temperature on moisture sorption at 25% and 65% RH

For each of the materials the change in temperature results in a change in mass. However, for Limestone, there is a seemingly negligible difference with increasing temperature, but the difference between the change in mass from 23°C to 48°C represents a 36% drop in sorption capacity. This decrease in capacity over this range is observed for all of the materials with the exception of sandstone, but is most pronounced with the Karshif material where there is a 43% reduction. Over this range, it can be observed that there is no consistent trend in sorption capacity, with some materials absorbing the most moisture at 38 °C. This suggests the need to consider different environmental conditions during testing to allow for accurate design, and to account for the complex nature of differing materials' hygrothermal regulation performance.

## 412 7 CONCLUSIONS

413 This study has investigated the physical and chemical properties of three common vernacular  
414 building stones. These include sandstone and limestone, common to desert regions in many  
415 parts of the world, and Karshif, which is unique to the Siwa Oasis at the Western Desert of  
416 Egypt.

417 In contrast to the local understanding of limestone, which suggests that it is unsuited to  
418 buildings because of its poor thermal properties, it is shown that limestone has better thermal  
419 properties than both sandstone and Karshif, but limited hygric properties. This finding may  
420 explain the local experience of limestone as providing less thermal comfort than the other two  
421 stones, due to its lower capacity for moisture regulation.

422 Karshif's sensitivity towards moisture has been attributed to its high salt content. Indeed,  
423 under extreme conditions of high humidity, this material undergoes partial dissolution.  
424 However, testing under the hot and dry conditions normally found in the region of Siwa  
425 Oasis, it is demonstrated that it is a viable building material that exhibits good moisture  
426 regulation behavior. Similar behavior is also observed for the third tested material, sandstone.  
427 Hence, our results support the use of sandstone and Karshif for moisture buffering in  
428 buildings.

429 Rain in dry desert areas is a source for ground water and crop irrigation, but is also an agent of  
430 building deterioration. Hence, building materials within this region have to withstand these  
431 atypical extreme weather events. Therefore, local materials need to be utilised within carefully  
432 designed wall assemblies or treated wall sections and, in the case of Karshif, not used in areas  
433 where RH regularly reaches 80%. Without this, there is a risk of a shift towards concrete or  
434 other modern materials which, though durable, carry heavy negative environmental impacts.

435 Methodologically, it is shown that the use of standardised testing conditions for vernacular  
436 materials may paint an incorrect picture of their true performance. For example, it was  
437 observed the partial dissolution of Karshif at regionally atypical relative humidities, and even  
438 a variation in performance under non-isothermal and non-isobaric conditions. However, a  
439 much clearer picture of true performance was obtained under test conditions typical of the  
440 regions from which the material was sourced. Hence, it is suggested that the environmental  
441 performance of vernacular materials is tested within the environmental context they are likely  
442 to experience under true conditions, rather than adopting standard conditions which may be  
443 atypical in use.

444 Overall, the importance of considering the moisture properties of building materials in  
445 addition to their thermal properties is clearly demonstrated. In fact, the only explanation for  
446 the local perception of limestone as a building material that produces lower internal comfort –  
447 despite its superior thermal properties to both sandstone and Karshif – is through our  
448 demonstration of the latter materials' superior hygric properties. Hence, differences in  
449 moisture sorption behaviour have the potential to impact the indoor environment and the  
450 energy use of buildings. It is therefore critical for designers to understand the impact that the  
451 choice of materials has on the comfort of occupants and building energy performance.

452

## 453 8 ACKNOWLEDGEMENTS

454 This research is supported by Newton-Mosharafa Fund under PhD joint supervision scheme  
455 and EPSRC Centre for Decarbonisation of the Built Environment (dCarb) [grant number  
456 EP/L016869/1]. Authors are thankful for the cooperation of lab technicians at Bath  
457 University. Thanks to Ms Shaghayegh Mohammad for her support in recording final data.

458 Also thanks should go to local community of Gara Oasis, particularly Mr Soliman Mohamed,  
459 who facilitated the transportation of materials from this remote area.

460

## 461 9 REFERENCES

- 462 [1] Osanyintola, O. F., & Simonson, C. J. (2006). Moisture buffering capacity of hygroscopic  
463 building materials: Experimental facilities and energy impact. *Energy and Buildings*, 38,  
464 1270–1282. <http://doi.org/10.1016/j.enbuild.2006.03.026>
- 465 [2] Walker, P., Thomson, A., & Maskell, D. (2017). To Your Health: health benefits of  
466 natural building materials.
- 467 [3] Fosas, D., Albadra, D., Natarajan, S., & Coley, D. A. (2018). Refugee housing through  
468 cyclic design. *Architectural Science Review*, 61(5), 327-337.
- 469 [4] Makhoulf, N. N. (2013). *Towards an Integrated Neo-vernacular Built Environment:  
470 Design guidelines for the living environments inspired by socio-cultural and  
471 environmental aspects, Qārrat 'Um-Āṣāḡīr Village, The Western Desert of Egypt.*  
472 Stuttgart university and Ain-Shams University.
- 473 [5] Al-Taweel, H. (1988). *Environment and Architecture in Siwa* (master's thesis). Alexandria  
474 University.
- 475 [6] Cagnon, H., Aubert, J. E., Coutand, M., & Magniont, C. (2014). Hygrothermal properties  
476 of earth bricks. *Energy and Buildings*, 80, 208–217.  
477 <http://doi.org/10.1016/j.enbuild.2014.05.024>
- 478 [7] Cascione, V., Maskell, D., Shea, A., and Walker, P. (2019). A review of moisture  
479 buffering capacity: From laboratory testing to full-scale measurement. *Construction and  
480 Building Materials*, 200:333 – 343.
- 481 [8] Zhai, Z. (John), & Previtali, J. M. (2010). Ancient vernacular architecture: characteristics  
482 categorization and energy performance evaluation. *Energy and Buildings*, 42(3), 357–  
483 365. <http://doi.org/10.1016/j.enbuild.2009.10.002>
- 484 [9] Dabaieh, M. (2011). *A Future for the Past of Desert Vernacular Architecture: Testing a  
485 Novel Conservation Model and Applied Methodology in the Town of Balat in Egypt.*  
486 Lund University.
- 487 [10] Mcgregor, F., Heath, A., Maskell, D., Fabbri, A., & Morel, J. (2016). A review on the  
488 buffering capacity of earth building materials. *Proceedings of the Institution of Civil  
489 Engineers Construction*, 169(CM5), 241–251.
- 490 [11] Abdel-Motelib, A., Taher, A., & El Manawi, A. H. (2015). Composition and diagenesis  
491 of ancient Shali city buildings of evaporite stones (kerchief), Siwa Oasis, Egypt.  
492 *Quaternary International*, 369, 78–85. <http://doi.org/10.1016/j.quaint.2014.09.009>
- 493 [12] Dabaieh, M., Makhoulf, N. N., & Hosny, O. M. (2016). Roof top PV retrofitting: A  
494 rehabilitation assessment towards nearly zero energy buildings in remote off-grid  
495 vernacular settlements in Egypt. *Solar Energy*, 123, 160–173.  
496 <http://doi.org/10.1016/j.solener.2015.11.005>
- 497 [13] Sallam, E. S., Abd El-aal, A. K., Fedorov, Y. A., Bobrysheva, O. R., & Ruban, D. A.  
498 (2018). Geological heritage as a new kind of natural resource in the Siwa Oasis , Egypt :  
499 The first assessment , comparison to the Russian South , and sustainable development  
500 issues. *Journal of African Earth Sciences*, 144, 151–160.  
501 <http://doi.org/10.1016/j.jafrearsci.2018.04.008>

- 502 [14] Rovero, L., Tonietti, U., Fratini, F., & Rescic, S. (2009). The salt architecture in Siwa  
503 oasis – Egypt (XII–XX centuries). *Construction and Building Materials*, 23(7), 2492–  
504 2503. <http://doi.org/10.1016/j.conbuildmat.2009.02.003>
- 505 [15] Farrag, A. E. hay A., El Sayed, E. S. A., & Megahed, H. A. (2016). Land Use / Land  
506 Cover Change Detection and Classification using Remote Sensing and GIS Techniques :  
507 A Case Study at Siwa Oasis , Northwestern Desert of Egypt. *International Journal of*  
508 *Advanced Remote Sensing and GIS*, 5(3), 1649–1661.
- 509 [16] CAPMAS. (2016). *Egypt Statistical Yearbook 2016, SECTION (1): Geography and*  
510 *Climate* (Vol. 107).
- 511 [17] IAMAT. (2015). Climate Information by City. Retrieved May 7, 2018, from  
512 <https://www.iamat.org/country/egypt/climate-data#null>
- 513 [18] Brunauer, S., Emmett, P. H., & Teller, E. (1938). Adsorption of gases in multimolecular  
514 layers. *Journal of the American chemical society*, 60(2), 309-319.
- 515 [19] Liuzzi, S., Rubino, C., Stefanizzi, P., Petrella, A., Boghetich, A., Casavola, C., &  
516 Pappalettera, G. (2018). Hygrothermal properties of clayey plasters with olive fibers.  
517 *Construction and Building Materials*, 158, 24–32.  
518 <http://doi.org/10.1016/j.conbuildmat.2017.10.013>
- 519 [20] Rode, C., Peuhkuri, R., Mortensen, L. H., Hansen, K. K., Time, B., Gustavsen, A., ...  
520 Arfvidsson, J. (2005). *Moisture Buffering of Building Materials*.
- 521 [21] Joussein, E., Sciences, E., De, Â. C., Bag, P., North, P., & Zealand, N. (2005). Halloysite  
522 clay minerals ÿ a review d. *Clay Minerals*, 40, 383–426.  
523 <http://doi.org/10.1180/0009855054040180>
- 524 [22] Meunier, A. (2005). *Clays*. Springer Science & Business Media.
- 525 [23] Petruccioli, A., & Montalbano, C. (2011). *Siwa Oasis: Actions for a sustainable*  
526 *development*. (A. Petruccioli & C. Montalbano, Eds.). Bari: DICAR. Retrieved from  
527 <http://architettura.poliba.it>
- 528 [24] Orabi, H., Beshtawy, M. El, Osman, R., & Gadallah, M. (2015). Larger benthic  
529 foraminiferal turnover across the Eocene – Oligocene transition at Siwa Oasis , Western  
530 Desert , Egypt *Journal of African Earth Sciences* Larger benthic foraminiferal turnover  
531 across the Eocene – Oligocene transition at Siwa Oasis , Western . *Journal of African*  
532 *Earth Sciences*, 105(August), 85–92. <http://doi.org/10.1016/j.jafrearsci.2015.03.002>
- 533 [25] Ostroff, A. (1964). Conversion of gypsum to anhydrite in aqueous salt solutions.  
534 *Geochimica et Cosmochimica Acta*, 28(9), 1363--1372.
- 535 [26] Mathlouthi, M., & Rogé, B. (2003). Water vapour sorption isotherms and the caking of  
536 food powders. *Food Chemistry*, 82(1), 61–71. [http://doi.org/10.1016/S0308-](http://doi.org/10.1016/S0308-8146(02)00534-4)  
537 [8146\(02\)00534-4](http://doi.org/10.1016/S0308-8146(02)00534-4)
- 538 [27] Maskell, D., Thomson, A., & Walker, P. (2018). Multi-criteria selection of building  
539 materials. *Proceedings of the Institution of Civil Engineers: Construction*  
540 *Materials*, 171(2), 49-58. <https://doi.org/10.1680/jcoma.16.00064>
- 541 [28] Sing, K. S. W., Everett, D. H., Haul, R. A. W., Moscou, L., Pierotti, R. A., Rouquerol, J.,  
542 & Siemieniewska, T. (1985). *Reporting physisorption data for gas/solid systems — with*  
543 *special reference to the determination of surface area and porosity The purpose*. *Pure &*  
544 *Applied Chemistry* (Vol. 57).
- 545 [29] Umprayn, K., Mendes, R.W. (1987). Hygroscopicity and Moisture Adsorption Kinetics

- 546 of Pharmaceutical Solids: A Review. *Drug Development and Industrial Pharmacy* 13,  
547 653-693.
- 548 [30] van der Wel, G.K., Adan, O.C.G. (1999). Moisture in organic coatings — a review.  
549 *Progress in Organic Coatings* 37, 1-14.
- 550 [31] Basu, S., Shivhare, U.S., Mujumdar, A.S. (2006). Models for Sorption Isotherms for  
551 Foods: A Review. *Drying Technology* 24, 917-930.
- 552 [32] Vivian, C. (2007). *The western desert of Egypt: An explorer's handbook*. Cairo, Egypt:  
553 American University in Cairo Press.
- 554 [33] Makhlof, N. N., & Eid, Y. Y. (2013). Towards an Integrated Neo-vernacular Living  
555 Environment: physical and socio-cultural aspects. In *Democratic Transitions and*  
556 *Sustainable Communities: Overcoming Challenges through innovative practical*  
557 *solutions* (pp. 238–250). Cairo, Egypt: SB13 Cairo.